BNL--41669

DE88 016730

CONF-880704--5

BNL-41669

Magnetic correlations in UPt$_3$ and U$_{1-x}$Th$_x$Pt$_3$

G. Aeppli and E. Bucher
AT&T Bell Laboratories, Murray Hill, NJ 07974, U.S.A.

A.I. Goldman[a] and G. Shirane
Brookhaven National Laboratory, Upton, NY 11973, U.S.A.

C. Broholm and J.K. Kjems
Risø National Laboratory, DK-4000 Roskilde, Denmark

Abstract

Neutron scattering experiments on UPt$_3$ and U$_{1-x}$Th$_x$Pt$_3$ are reviewed. At relatively high energies (~ 5 meV), the magnetic fluctuation spectrum is modulated by the structure factor derived from short-range antiferromagnetic correlations where the two U ions in each unit cell are oppositely polarized. In contrast, at low energies ($\leq$ 1 meV), the diffuse inelastic scattering is associated with antiferromagnetic correlations where the unit cell is doubled. Nominally pure UPt$_3$ exhibits magnetic order with the wavevector corresponding to this doubling and a static moment of $0.02 \pm 0.01\ \mu_B$. (U$_{1-x}$Th$_x$)Pt$_3$ with $x \simeq 0.05$ exhibits ordering of the same type, but with a much larger static moment, $0.65 \pm 0.1\ \mu_B$. Neutron scattering measurements on UPt$_3$ with implications for superconductivity are surveyed.

(a) Current address: Ames Laboratory, Iowa State University, Ames IA 50011, U.S.A.

Keywords: heavy fermions, superconductivity, antiferromagnetism, Fermi liquid.

I. Introduction

Because of its many unusual properties and the availability of large single crystals, UPt_3 has been studied more than any other heavy fermion system[1-6]. Even so, almost each new experiment has provided another surprise. This is true of both seemingly routine measurements, such as determinations of upper critical fields[3], and more exotic experiments, such as torsional oscillator studies[4] of flux lattice phenomena. Even though most of the effort has been devoted to bulk properties, some microscopic measurements have also been performed and have yielded their share of surprises. We describe here the results obtained by one microscopic technique, namely neutron scattering.

The paper is organized as follows. We first provide some details about the neutron scattering techniques employed. The next three sections are devoted to inelastic measurements at relatively high energies, magnetic Bragg scattering in $U_{1-x}Th_xPt_3$ and the related low energy scattering in UPt_3, and neutron scattering experiments relating to superconductivity, respectively. Finally, section VI contains a summary and discussion of future possibilities.

II. Neutron scattering experiments

The magnetic neutron scattering cross-section is proportional to the Fourier transform $S(Q,\omega)$ of the correlation function formed between pairs of moments in the material of interest. For ordered crystals, the elastic portion of this scattering consists of magnetic Bragg peaks, while the inelastic scattering is related to the generalized magnetic susceptibility $\chi(Q,\omega)$ via the fluctuation-dissipation theorem:

$$\frac{\partial^2\sigma}{\partial\Omega\partial\omega} = \frac{\chi''(Q,\omega)}{\pi}\gamma_0^2|F_Q|^2(1-\exp-\beta\hbar\omega)^{-1} \qquad (1)$$

where Q represents the momentum transfer, $\hbar\omega$ the energy transfer, $|F_Q|^2$ the electronic form-factor and $\chi''(Q,\omega)$ the imaginary part of $\chi(Q,\omega)$.

The instruments used for our unpolarized studies were triple-axis spectrometers located at thermal beam ports of the Brookhaven National Laboratory High Flux Beam Reactor and in the cold-neutron guide hall of the Risø National Laboratory DR3 reactor. Monochromators and analyzers were pyrolitic graphite (PG) crystals set for their (002) reflections; PG, Be and BeO filters eliminated higher-order contamination of the beams and reduced the elastic scattering admitted by the analyzer at nominally finite energy transfers. We performed polarized beam measurements using the Brookhaven triple-axis instrument H8, with vertically magnetized Cu_2MnAl crystals in the monochromator and analyzer positions, and a flipping coil between the sample and analyzer. The data reported are the differences between the number of spin-flip events observed with the neutron polarization oriented parallel (HF) and perpendicular (VF) to the momentum transfers.

Single crystals, 6 mm in diameter and 1-2 cm in length, were produced by the float-zone method. They were mounted singly or in larger groups (of up to five) on the cold fingers of various pumped ^4He, pumped ^3He, and ^3He-^4He dilution cryostats. The $(h,0,\ell)$ zones of the hexagonal close-packed crystals (space group $P6_3/mmc$ coincided with the horizontal scattering plane of the instruments. The components h and ℓ are measured in units of $a^* = 4\pi/\sqrt{3}a = 1.26$ Å^{-1} and $c^* = 2\pi/c = 1.28$ Å^{-1}. Fig. 1(a) shows the arrangement of the U atoms in UPt_3.

III. Medium- and high-energy fluctuations

Our original measurements[5] on UPt_3 were done on a polycrystalline sample. Because momentum selection rules could not be used to avoid phonon scattering, polarized beam spectroscopy was performed. Fig. 2 shows some of the results. The principal conclusions are that the energy scale for the fluctuations is $\hbar\Gamma \approx 10$ meV, while the scattering cross-section, expressed in absolute units is in agreement with bulk susceptibility data. In particular, the integral $\int_{-\infty}^{+\infty}[\partial^2\sigma/\partial\Omega\partial\omega]\partial\omega$, which measures the size μ_{eff} of the fluctuating moments, was found approximately by summing the spectrum in Fig. 1 to 38 meV. The corresponding μ_{eff} at 1.3 K is $2.1 \pm 0.4\ \mu_B$, not far from values deduced from the high-temperature Curie constant[6]. Furthermore, a Kramers-Kronig transform of the data yields a real zero-frequency susceptibility of $0.3 \pm 0.1\ \mu_B^2/\mathrm{meV}$, consistent with the low-temperature bulk value (χ_0) of $0.26\ \mu_B^2/\mathrm{meV}$[6].

The result that the 10 meV characteristic energy is of the same order as the Fermi energy deduced from various bulk measurements, and the continuum nature of the scattering suggested that $S(Q,\omega)$ for UPt_3 might be of the form expected for simple Fermi liquids[7]. Obviously, our powder-averaged data, while consistent with simple theory, could not be used to establish the Q-dependence of

$S(Q,\omega)$. Therefore, we undertook an investigation of single crystals[8]. Both constant-energy and constant-Q scans were performed to determine correlations between moments at different sites and energy spectra, respectively. Fig. 3 shows that there is a maximum in the scattering at $Q = (0,0,1)$. Similar are maxima located at $(2,0,\pm 1)$, which implies that on the time scales probed (10^{-12} s), nearest neighbor moments (i.e. those located at neighboring open and filled vertices in Fig. 1(a)) are correlated antiferromagnetically. This result could be interpreted as a manifestation of the Pauli principle in a Fermi liquid, were it not for the constant-Q scans (see Fig. 5) at (0,0,2) - a Brillouin zone center equivalent to (0,0,0) - which show substantial magnetic continuum scattering over the entire frequency range probed. A Kramers-Kronig analysis demonstrates that the scattering accounts for the entire bulk susceptibility χ_0 to within possible systematic errors of 20%. This result is very surprising because for simple Fermi liquids (see Fig. 3), there should be no scattering at finite frequencies for $Q = 0$; that χ_0 is non-zero follows since the position of the peak in $S(Q,\omega)$ for a Fermi liquid moves linearly to $\omega = 0$ as $Q \rightarrow 0$. It is even more remarkable in light of the visibility of de Haas-van Alphen oscillations in UPt_3 [9] and the correspondence between de Haas-van Alphen and neutron data in weak itinerant (transition metal) ferromagnets[10].

In addition to energy scans at $Q = (0,0,2)$, Fig. 4 shows scans at (0,0,1), the location of a principal peak in the constant-$\hbar\omega$ scans. The essential result is that the difference between the two scans, even at relatively high energies (≥ 5 meV), becomes substantial only for $T < 20$ K. The inset shows the outcome of a Kramers-Kronig analysis of the data: note that the gentle maximum observed at 17 K in the bulk χ_0 (dashed curve) occurs near the appearance of antiferromagnetic correlations as measured by χ_Q for $Q = (0,0,1.01)$.

IV. $U_{1-x}Th_xPt_3$ and low frequency excitations in UPt_3

After the discovery (by specific heat, resistivity, and bulk susceptibility measurements) of a phase transition at ≥ 5 K in $U_{1-x}Th_xPt_3$ and $U(Pt_{1-x}Pd_x)_3$ for $x \geq 0.03$, we performed a neutron scattering experiment on a single crystal of $U_{0.95}Th_{0.05}Pt_3$[12]. A search of the $(h,0,\ell)$ zone at low temperatures revealed no magnetic Bragg peaks at the reciprocal lattice points, such as (0,0,1) and $(2,0,\pm 1)$, at which the inelastic scattering described in section III was peaked. Instead, magnetic reflections occurred at points of the form $(h+\frac{1}{2},0,\ell)$, where h and ℓ are integers. Particularly strong reflections were located at $(\pm\frac{1}{2},0,1)$ and $(\pm\frac{1}{2},0,2)$. In contrast to the ordered structure that would be associated with the short-lived correlations of Section II, the superlattice for $U_{0.95}Th_{0.05}Pt_3$ involves a doubling of the unit cell in the basal plane, as shown in Fig. 1(b). As for other heavy electron magnets, the ordered moment (0.65 ± 0.1 μ_B U *atom*) is well below that (2-3 μ_B) found both in high-temperature bulk susceptibility and our low-temperature inelastic neutron scattering measurements (see Section II). Nevertheless, as seen in Fig. 5, the magnetic order evolves quite conventionally below the Néel temperature of 6.5 K. Frings, Renker, and Vettier have obtained similar results for $U(Pt_{1-x}Pd_x)_3$[13].

Having found that $U_{0.95}Th_{0.05}Pt_3$ displays magnetic Bragg peaks at reciprocal lattice points with half-integer in-plane indices, we set out to probe the elastic and inelastic scattering near such points in nominally pure crystals of UPt_3[14]. Fig. 3 shows that the $(\xi_\parallel,0,1)$ constant-$\hbar\omega$ scan changes dramatically as $\hbar\omega$ is reduced from 8 to 0.5 meV. The maximum at (001) disappears, and two new maxima appear at $(\pm\frac{1}{2},0,1)$, as expected given the results for $U_{0.95}Th_{0.05}Pt_3$. More surprising is that there are also small elastic ($\hbar\omega = 0$) peaks at $(\pm\frac{1}{2},0,1)$. The corresponding ordered moment is 0.02 ± 0.01 μ_B, which is consistent with an anomalous muon spin relaxation signal seen previously for UPt_3 at low temperatures[15]. Fig. 8 shows the temperature dependence of the elastic scattering at $Q = (\frac{1}{2},0,1)$, which is quite different than for $U_{0.95}Th_{0.05}Pt_3$ (compare Figs. 5 and 6) in that it rises nearly linearly with decreasing temperature over a large range of $T < T_N \simeq 5$ K. Fig. 2(b) shows that $S(Q,\omega)$, measured with Q displaced slightly from the ordering vector to eliminate Bragg contamination, has a maximum near T_N. This is expected for conventional magnets undergoing second order phase transitions: the decrease for $T < T_N$ is associated with a reduction in the fluctuating moment as the system becomes progressively more ordered.

V. Superconductivity

There is considerable experimental[1-4] and theoretical[16] work which suggests that the superconductivity is due to the formation of unconventional (i.e. not BCS-type singlet) electron pairs via exchange of magnetic fluctuations.

In this regard, an interesting finding[14] has been that, as shown in Fig. 7, the characteristic energy for magnetic fluctuations with $Q = (\pm\frac{1}{2},0,1)$ in nominally pure UPt_3 is 0.2 meV, of the same magnitude as the pair-breaking energy associated with $T_c = 0.5$ K[17]. A related result is that the static magnetic order parameter ceases to rise as T is reduced through T_c. Work to study both elastic and inelastic scattering at temperatures well below T_c is currently underway[18]. Finally, we note that polarized neutron diffraction has shown that the magnetic moment induced by an external field does not change when UPt_3 becomes a superconductor[19]. This is in contrast to what occurs for ordinary superconductors such as V_3Si[20], where the reduction in the induced moment corresponds directly to the spin part of the magnetic susceptibility (the orbital part is not affected by the phase transition).

VI. Discussion and conclusions

We have shown that neutron scattering has provided many useful insights concerning the anomalous bulk properties of UPt_3. Notably, the successive appearance of two different types of antiferromagnetic correlations, with different characteristic energies, account for the maximum[4] in χ_0 for $T \approx 17$ K and the anomalies in various derivatives of the resistivity for $T \approx 5$ K[21]. Furthermore, while the data clearly exclude simple paramagnon models for UPt_3, they show UPt_3 to be much closer to an antiferromagnetic instability than previously supposed. In addition, they lend support to theories[16] where the pairing in the superconducting state is mediated by antiferromagnetic fluctuations.

In spite of the large progress made towards understanding UPt_3, many open questions remain. Firstly, it is unclear whether the magnetic order found for nominally pure UPt_3 is intrinsic. Because the Bragg-like magnetic scattering is not resolution-limited[14], some disorder must be present even in our nominally pure samples, which by most standards (e.g. chemical and sharpness of superconducting T_c) are exceptionally clean. A second issue is the current lack of agreement between detailed calculations[22] of $S(Q,\omega)$ and the experimental results. In general, the calculations yield distinguishable Fermi liquid and interband contributions, with the latter always accounting for a considerably smaller fraction of χ_0 than the data taken for $Q = (0,0,2)$. Finally, even though theoretical predictions are available[23], relatively few scattering data have been collected for the superconducting state. In view of the many unanswered questions about UPt_3, we are looking forward to some more surprises.

ACKNOWLEDGEMENTS

We are grateful to B. Batlogg, D. Bishop, Z. Fisk, P. Frings, R. Joynt, C. Pethick, D. Pines, A. Ramirez, T.M. Rice, T. Rosenbaum, S. Shapiro, C. Vettier and especially C. Varma for helpful discussions. Work at Brookhaven National Laboratory was supported by the U.S. Dept. of Energy under Contract No. DE.AC02-76CH00016. One of us (G.A.) thanks both Risø and Brookhaven National Laboratories for their hospitality during the course of this work.

Figures

1 (a) The structure of UPt_3. Open and closed circles denote the positions of U atoms in adjacent basal planes, respectively. The planes are a distance c/2 apart.
(b) The magnetic structure of $U_{0.95}Th_{0.05}Pt_3$, $U(Pd_xPt_{1-x})_3$, and the nominal pure samples of UPt_3 used for the present study [from ref. 12].

2. Constant-Q polarized neutron scattering spectra for polycrystalline UPt_3. Solid and dashed lines are obtained from fits described in ref. 5 [from ref. 5].

3. Constant-$\hbar\omega$ scans for oriented single crystals of UPt_3. Lines are guides to the eye, ΔE denotes the incoherent energy resolutions (FWHM) of the instruments [from refs. 8 and 14].

4. Energy scans near allowed ($Q = (002)$) and forbidden ($Q = (001)$) nuclear Bragg points. Solid lines are obtained from fits described in ref. 8. Inset shows the temperature-dependent magnetic susceptibility deduced from fits to the data for the two momentum transfers; the dashed line represents bulk ($Q = 0$) susceptibility data [from ref. 8].

5. Temperature dependence of the magnetic Bragg intensity measured at $(\frac{1}{2},0,1)$ for $U_{0.95}Th_{0.05}Pt_3$ [from ref. 12].

6. Temperature dependence of (a) the intensity of the elastic peak at $Q = (\frac{1}{2}\ 0\ 1)$ and (b) the inelastic scattering at $Q = (0.52, 0, 0.99)$ for $\hbar\omega = 85$ µeV [from ref. 14].

7. (a) Constant-Q scans at $Q = (0.3,0,1)$ at $T = 0.5$ K and $Q = (0.53,0,1)$ at $T = 5$ K and 0.5 K.
(b) $\chi''(Q,\omega)$ at the same two temperatures deduced from data in (a) and eq. (1) [from ref. 14].

References

1. G.R. Stewart, Z. Fisk, J.O. Willis, and J.L. Smith, Phys. Rev. Lett. 52, 679 (1984).

2. D.J. Bishop, C.M. Varma, B. Batlogg, E. Bucher, J.L. Smith, and Z. Fisk, Phys. Rev. Lett. 53, 1009 (1984); D. Jaccard, T. Flouquet, P. Legay, and J.L. Tholence, J. Appl. Phys. 57, 3022 (1985).

3. B.S. Shivaram, T.F. Rosenbaum, and D.G. Hinks, Phys. Rev. Lett. 57, 1259 (1986).

4. R.N. Kleiman, P.L. Gammel, E. Bucher, and D.J. Bishop, preprint (1987).

5. G. Aeppli, E. Bucher, and G. Shirane, Phys. Rev. B32, 7579 (1985).

6. W.D. Schneider and C. Laubschat, Phys. Rev. B23, 997 (1981); P.H. Frings, J.J.M. Franse, F.R. de Boer, and A. Menovsky, J. Magn. Magn. Mat. 31-34, 240 (1983).

7. See, for example, D. Pines and P. Nozières, Quantum Liquids (Benjamin, N.Y. 1966) and C.J. Pethick, D. Pines, W.F. Quader, K.S. Bedell, and G.E. Brown, Phys. Rev. Lett. 57, 1955 (1986).

8. G. Aeppli, A. Goldman, G. Shirane, E. Bucher, and M.-Ch. Lux-Steiner, Phys. Rev. Lett. 58, 808 (1987); A.I. Goldman, G. Shirane, G. Aeppli, E. Bucher, and J. Hufnagl, Phys. Rev. B36, 8523 (1987).

9. L. Taillefer, R. Newbury, G.G. Lonzarich, Z. Fisk, and J.L. Smith, J. Magn. Magn. Mat. 63-64, 372 (1987).

10. G.G. Lonzarich, J. Magn. Magn. Mat. 54-57, 612 (1986).

11. A. de Visser, S.C.P. Klaase, M. van Sprang, J.J.M. Franse, A. Menovsky, and T.T.M. Palstra, J. Magn. Magn. Mat. 54-57, 375 (1986); G.R. Stewart, A.L. Giorgi, J.O. Willis, and J. O'Rourke, Phys. Rev. B34, 4629 (1986); A.P. Ramirez, B. Batlogg, A.S. Cooper, and E. Bucher, Phys. Rev. Lett. 57, 1072 (1986).

12. A.I. Goldman, G. Shirane, G. Aeppli, B. Batlogg, and E. Bucher, Phys. Rev. B34, 6564 (1986).

13. P.H. Frings, B. Renker, and C. Vettier, J. Magn. Magn. Mat. 63-64, 202 (1987).

14. G. Aeppli, E. Bucher, C. Broholm, J.K. Kjems, J. Baumann, and J. Hufnagl, Phys. Rev. Lett. 60, 615 (1988). P. Frings, B. Renker, and C. Vettier (unpublished) have also noted enhanced magnetic diffuse scattering and weak magnetic Bragg scattering at ($\frac{1}{2}$ 0 1) in nominally pure UPt_3.

15. R. Heffner, paper presented at International Conference on Valence Fluctuations (Bangalore, 1987).

16. K. Miyake, S. Schmitt-Rink, and C.M. Varma, Phys. Rev. B34, 6554 (1986); M.T. Béal-Monod, C. Bourbonnais, and V.J. Emery, Phys. Rev. B34, 7716 (1986); M.R. Norman, Phys. Rev. Lett. 59, 232 (1987); K. Machida and M. Kato, Phys. Rev. Lett. 58, 1986 (1987); C.M. Varma, Physica 148B, 17 (1987).

17. For theory which might be relevant, see A.J. Millis, S. Sachdev, and C.M. Varma, preprint (1988).

18. C. Broholm, D.J. Bishop, G. Aeppli, E. Bucher, N. Stücker, and K. Siemensmeyer, unpublished.

19. C. Stassis, J. Arthur, C.F. Majkrzak, J.D. Axe, B. Batlogg, J. Remeika, Z. Fisk, J.L. Smith, and A.S. Edelstein, Phys. Rev. B34, 4382 (1986).

20. C.G. Shull and F.A. Wedgwood, Phys. Rev. Lett. 16, 513 (1966).

21. A. de Visser, PhD. thesis, University of Amsterdam (1986).

22. See, e.g. A. Auerbach, J.H. Kim, and K. Levin, Physica 148B, 50 (1987).

23. R. Joynt and T.M. Rice, preprint (1988).

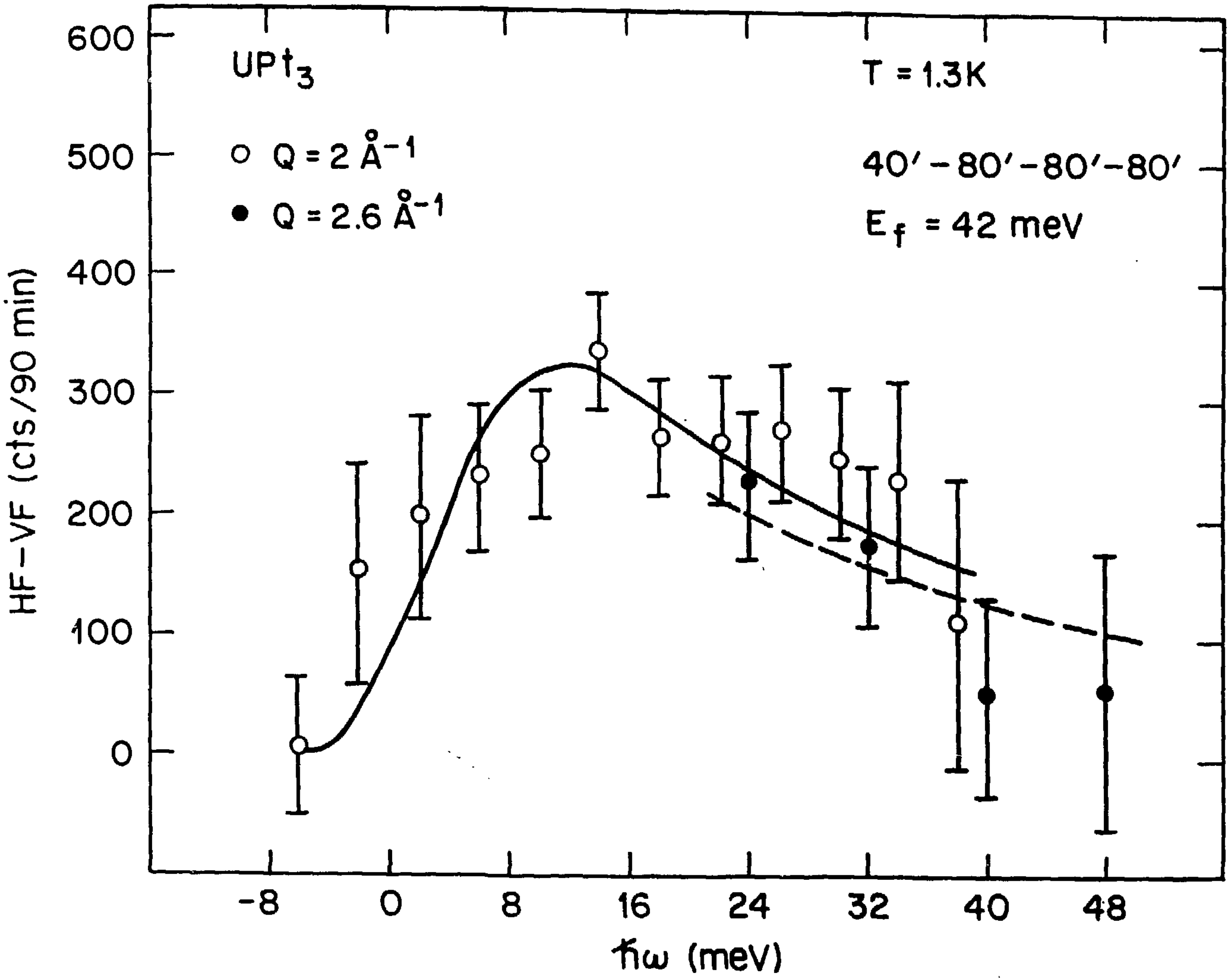
UPt$_3$
○ Q = 2 Å^{-1}
● Q = 2.6 Å^{-1}
T = 1.3K
40′ – 80′ – 80′ – 80′
E$_f$ = 42 meV
HF – VF (cts/90 min)
600
500
400
300
200
100
0
-8
0
8
16
24
32
40
48
ħω (meV)

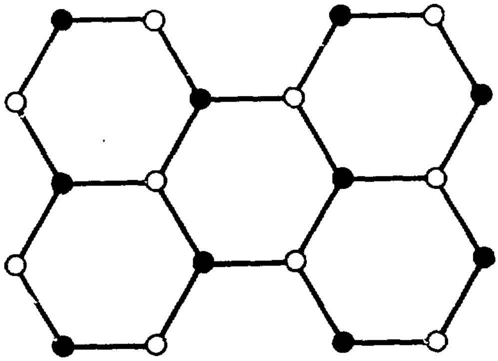

(a)

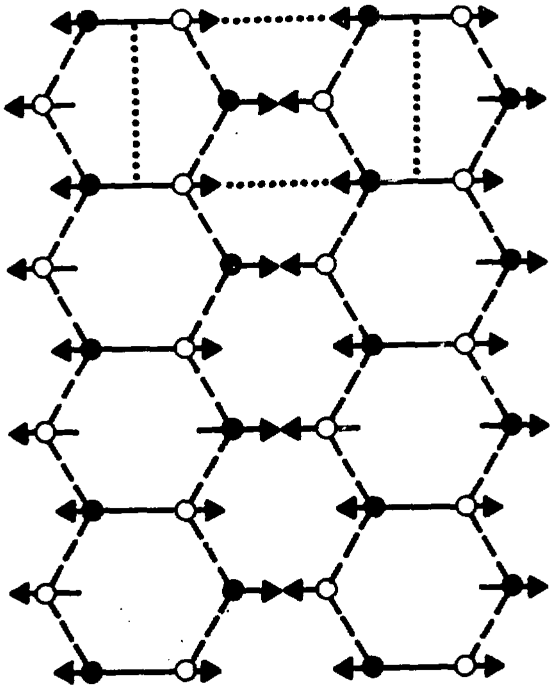

(b)

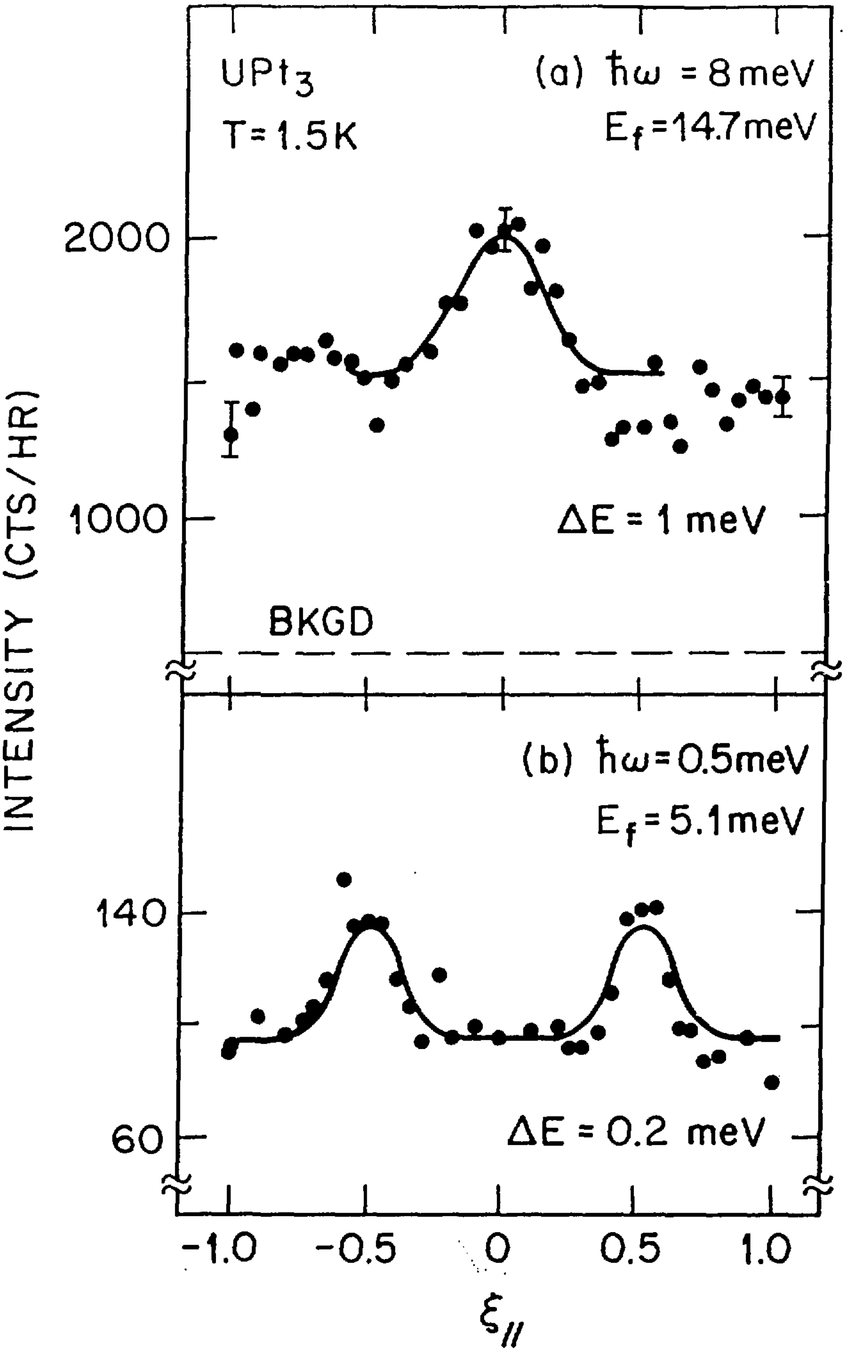
UPt$_3$
T = 1.5K
(a) ħω = 8 meV
E$_f$ = 14.7 meV
2000
1000
ΔE = 1 meV
BKGD
INTENSITY (CTS/HR)
(b) ħω = 0.5 meV
E$_f$ = 5.1 meV
140
60
ΔE = 0.2 meV
-1.0
-0.5
0
0.5
1.0
ξ$_{//}$

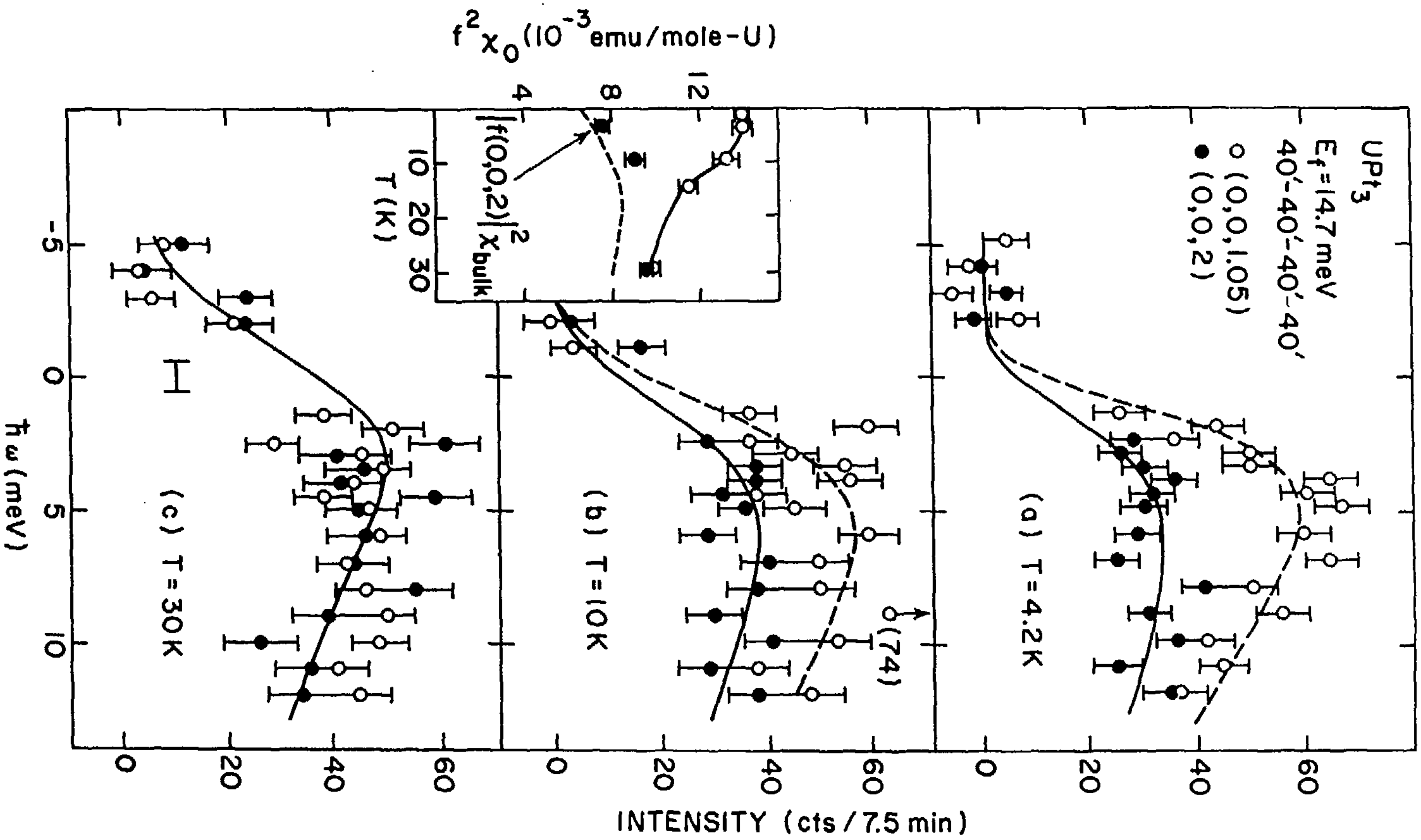
UPt$_3$
E_f=14.7 meV
40′-40′-40′-40′
○ (0,0,1.05)
● (0,0,2)
(a) T=4.2K
(b) T=10K
(c) T=30K
(74)
$f^2\chi_0$(10^{-3}emu/mole-U)
4
8
12
10 20 30
T(K)
$|f(0,0,2)|^2\chi_{bulk}$
-5
0
5
10
$\hbar\omega$(meV)
0
20
40
60
INTENSITY (cts/7.5 min)

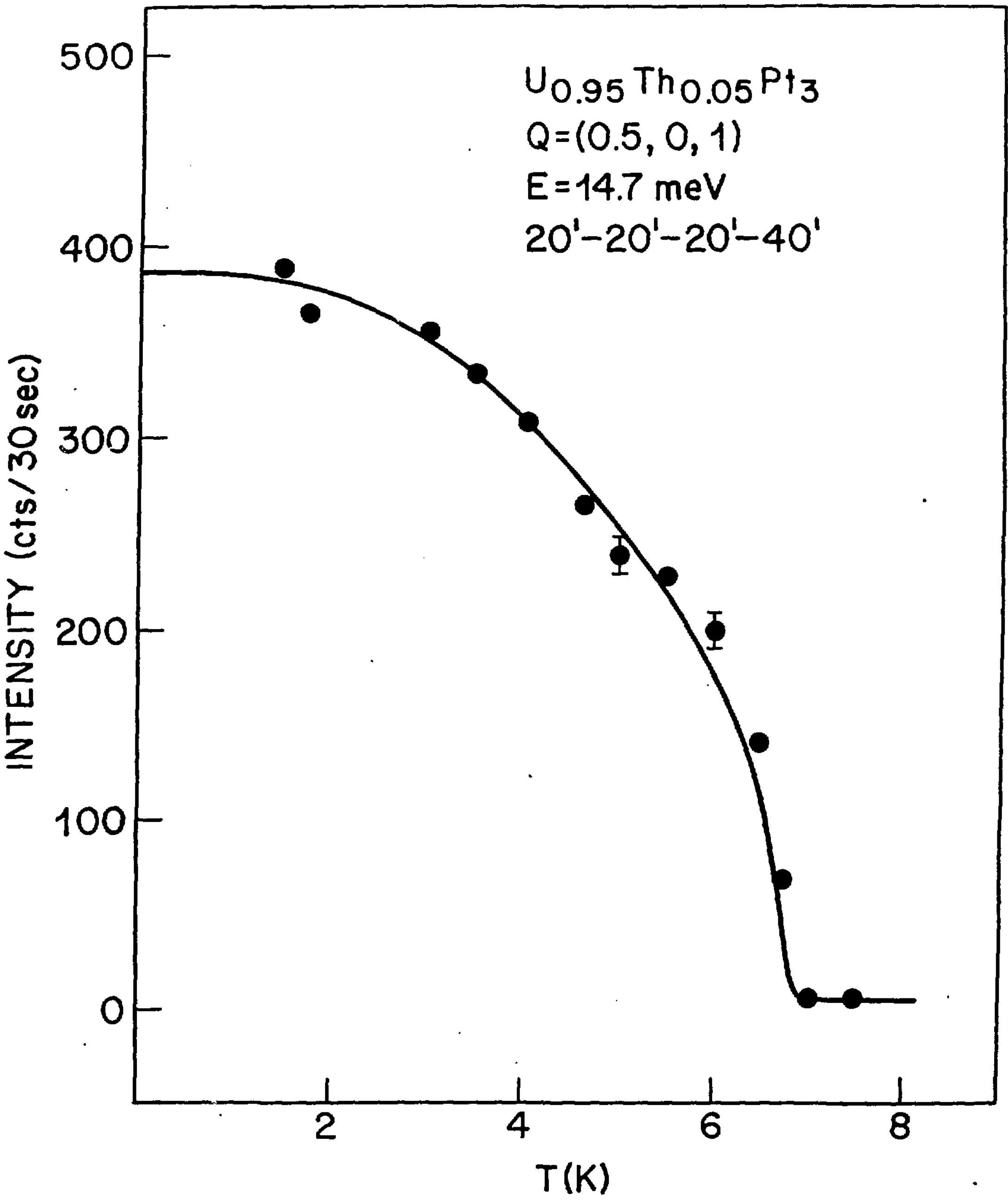
$U_{0.95}Th_{0.05}Pt_3$
Q=(0.5, 0, 1)
E=14.7 meV
20'-20'-20'-40'
INTENSITY (cts/30sec)
500
400
300
200
100
0
2
4
6
8
T(K)

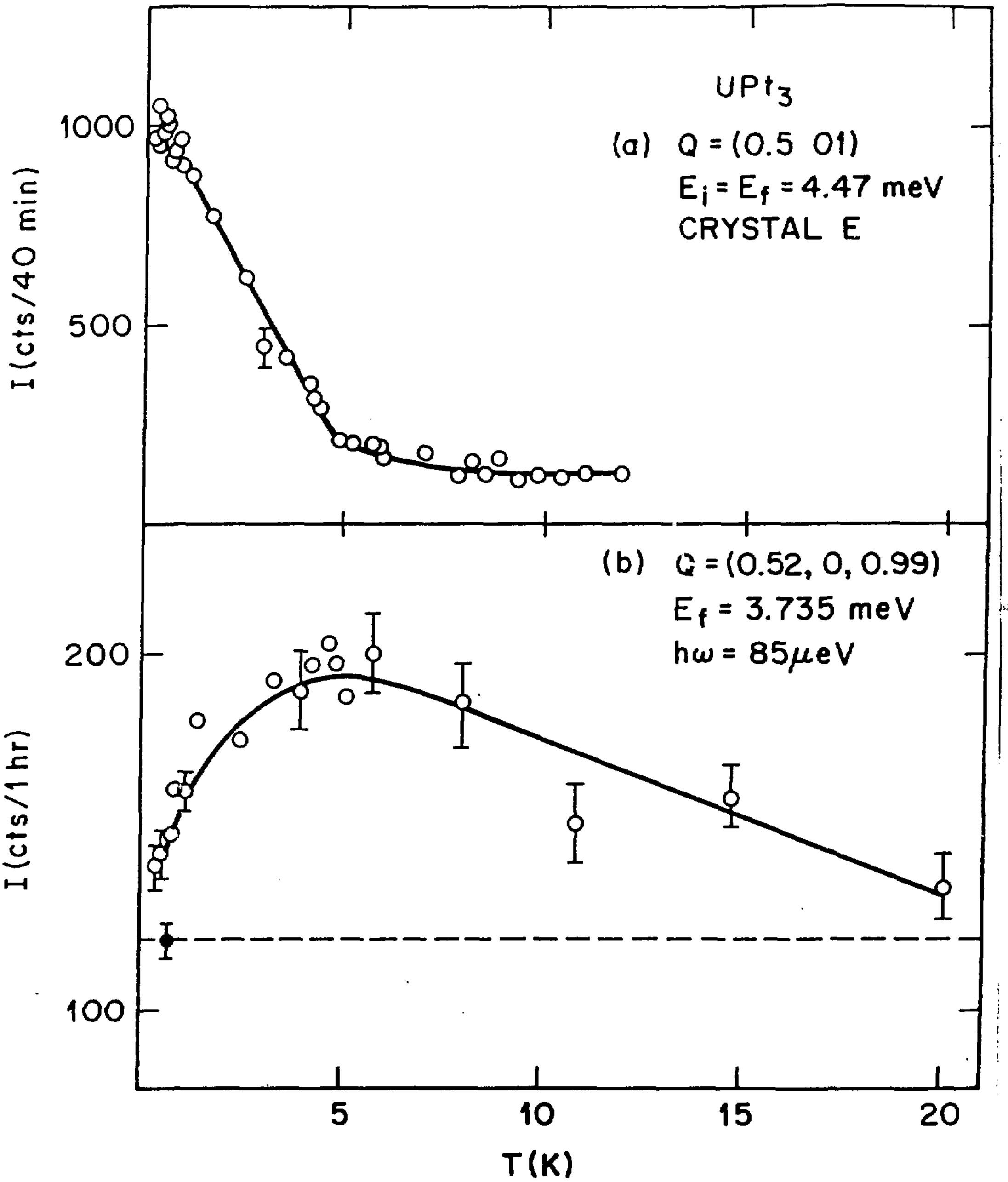
UPt$_3$
(a) Q = (0.5 01)
$E_i = E_f = 4.47$ meV
CRYSTAL E
I (cts/40 min)
1000
500
(b) Q = (0.52, 0, 0.99)
$E_f = 3.735$ meV
$h\omega = 85\mu$eV
I (cts/1 hr)
200
100
5
10
15
20
T(K)

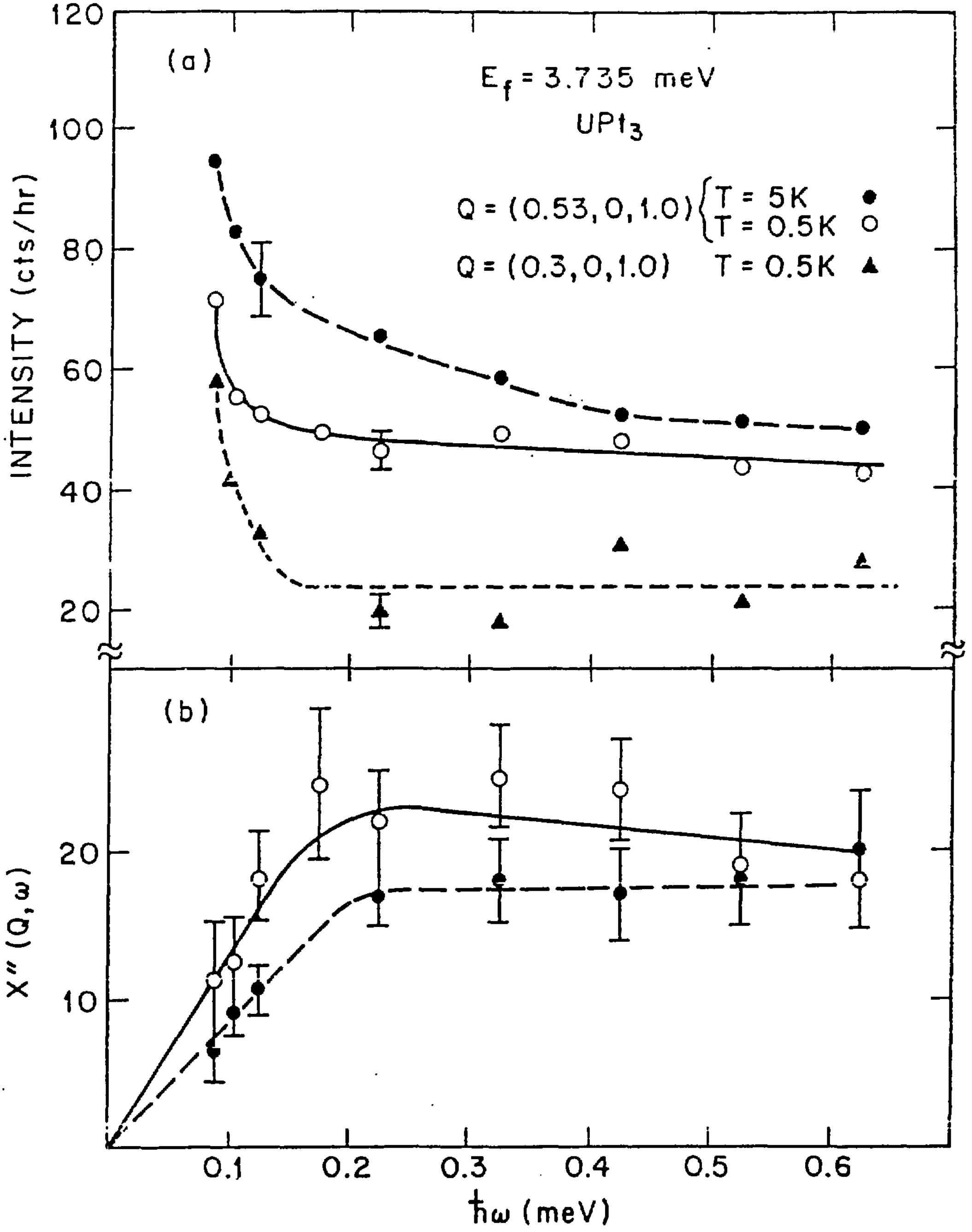
(a)
E_f = 3.735 meV
UPt3
Q = (0.53, 0, 1.0) { T = 5K ●
T = 0.5K ○
Q = (0.3, 0, 1.0) T = 0.5K ▲
INTENSITY (cts/hr)
120
100
80
60
40
20
(b)
X'' (Q, ω)
20
10
0.1
0.2
0.3
0.4
0.5
0.6
ħω (meV)